Supplementary Material 1: 2008 EV5's Radar Speckles

2008 EV5 Observations and Correlation

We observed EV5 on 2008 Dec 23 using nine of the ten VLBA stations in addition to the Green Bank Telescope (the VLBA station at Hancock, New Hampshire, was closed due to weather). The stations recorded data with a 62.5 kHz bandwidth centered at 2380.0 MHz (λ = 12.6 cm). The Arecibo transmissions were tuned so that the frequency in the frame of reference of the Earth's center-of-mass was constant at 2380 MHz. The correlator programs were set to account for the different Doppler shift at each station.

We processed the data both with a narrow-band software correlator written especially for this project and with the DiFX correlator program (Deller et al. 2007). DiFX has been used successfully in a wide variety of radio astronomy applications. However, the current version is limited in both minimum channel bandwidth and minimum integration time, and can only barely resolve radar speckle patterns. For EV5, the minimum integration time possible with DiFX was 0.325 s. In order to better resolve the speckles and to maximize the signal-to-noise ratio of our cross-correlations, we required the finer time resolution of the narrow-band correlator.

The two programs produce consistent output (Supplementary Figure 1). Downsampling the narrow-band output to the same time resolution produces a time series of echo power that matches that produced by DiFX to the level expected due to inevitable differences in the data binning. Recent upgrades to DiFX permit short integration times and narrower channels, so that speckle tracking is now a standard VLBA observing mode.

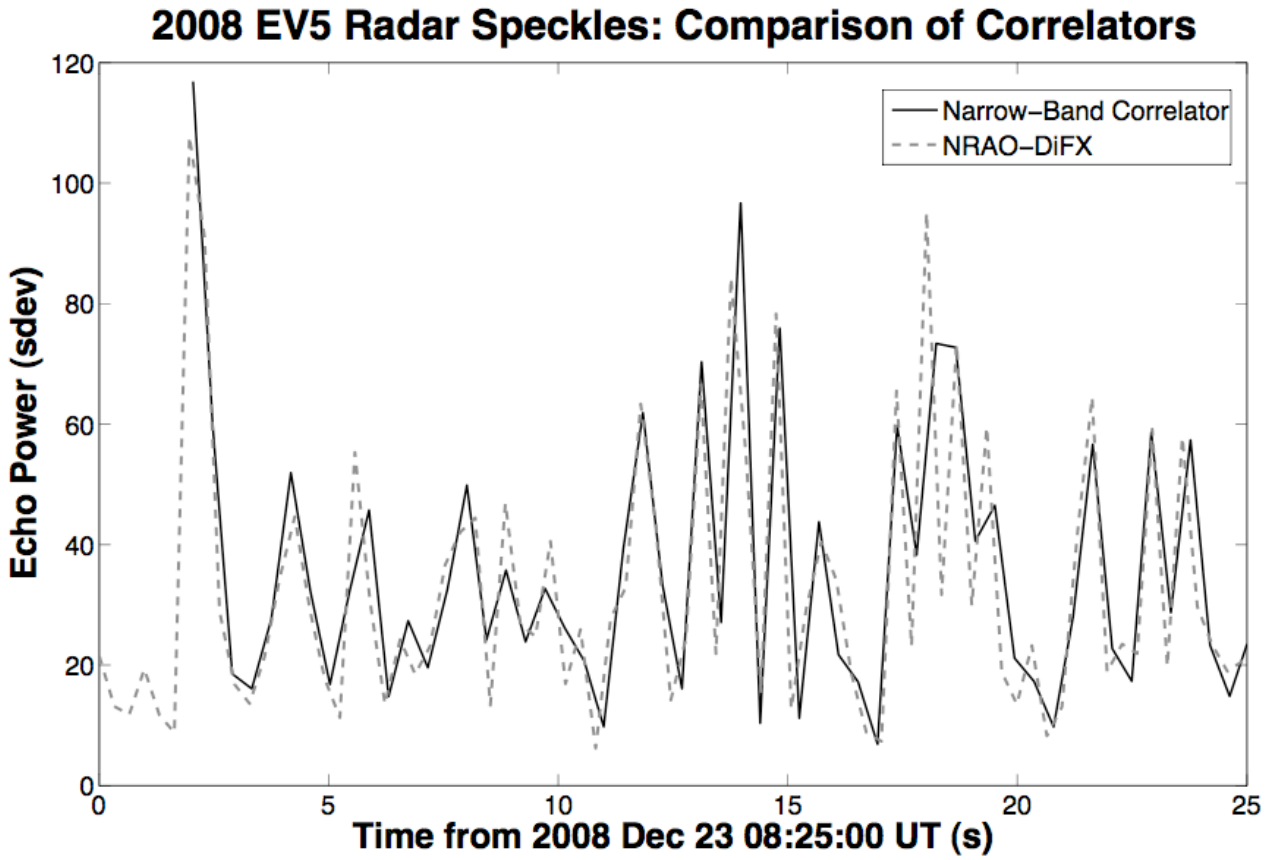

Supplementary Figure 1: The 2008 EV5 data from Green Bank on 2008 Dec 23 presented in Fig. 3 processed with time resolution of 0.325 s, computed with our narrow-band correlator and with DiFX. At this resolution, the speckles are only slightly resolved. The mismatches in amplitude are due to slight differences in the binning the data.

Properties of EV5's Speckle Pattern

Although its speckle pattern is uniquely determined by the shape and radar scattering properties of EV5's surface, in practice the pattern is indistinguishable from that of a randomly generated model surface. As a demonstration, consider the power spectrum of EV5's speckles as seen by GBT as compared to the power spectrum of a simulated series of speckles from a 450 m sphere with Lambertian scattering and random phase for each spot on the surface 1 wavelength (12.6-cm) across (Supplementary Fig. 2). For all scales larger than the speckle scale, the power spectrum of the speckles is flat. Below that scale (which λ/d puts at 2.8e-4 radians), the spectrum falls off steeply to the noise limit of the receiver.

The fall off is due to aliasing: variations in the speckle pattern at higher spatial frequency than the speckle scale require two lower frequencies to interfere with each other and higher orders

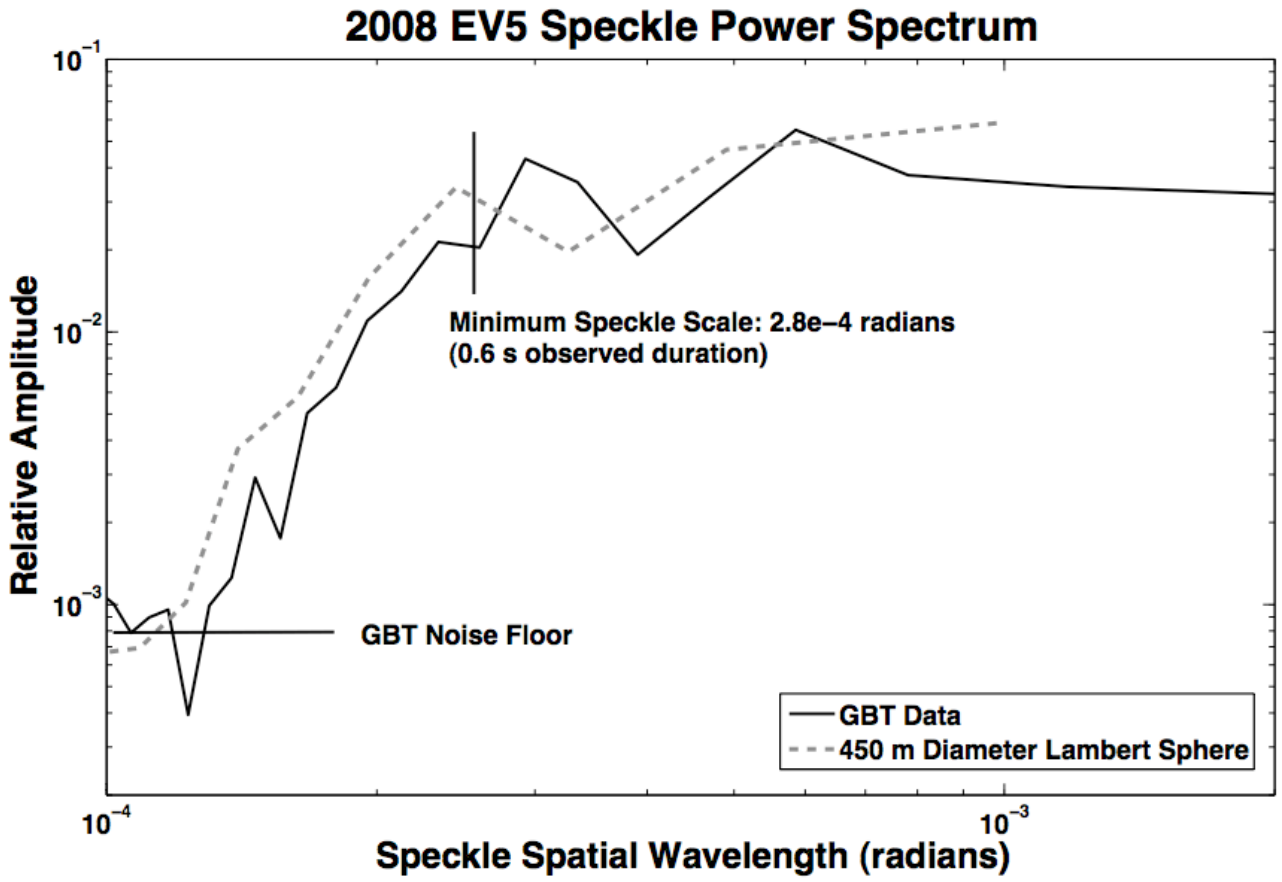

Supplementary Figure 2: Power spectrum of 2008 EV5 radar speckles as seen with Green Bank, and a simulated 450 m diameter sphere with Lambertian scattering and random phase. Speckle scale is measured in radians, obtained by specifying that the speckles move 2π radians in one 3.725 h rotation period. The flat spectrum for speckle scales larger than 2.8 x 10^{-4} radians is consistent with a rocky surface, the drop toward smaller spatial wavelengths is consistent with aliasing of large speckles, and the leveling off at speckle wavelengths less than about 10^{-4} is due to GBT's receiver noise. This spectrum contains 8 FFTs added together; point-to-point random variations are comparable to the amplitude.

of aliasing necessarily contain less and less power. EV5's speckle power spectrum may start to fall off at slightly longer wavelengths than the 450-m Lambert model, even though a 450-m sphere is a fairly close approximation to its shape. This is consistent with the radar scattering law inferred from the delay-Doppler data (cross-section ∝ $\cos^{2.4}$(incidence angle), Busch et al. 2010). EV5's echo is stronger at the center of the disc, due to the low incidence angle, so smaller separations and larger speckles contain somewhat more power.

On timescales longer than the speckle duration, the echo power measurements are not significantly correlated with each other, so that the long-wavelength spectrum is flat. The overall distribution of all of the measurements is well fit by a chi-square distribution with 1 degree of

freedom. That distribution is expected for a surface composed of a large number of elements reflecting with uniform random phases (e.g. a rocky surface that is rough on scales larger than millimeters). Each speckle can be considered as a measurement reflecting the sum of the phases from each point on the surface along particular lines of sight. If we consider points one wavelength apart, there are roughly 10^7 points on EV5. The vector addition of 10^7 randomly phased electric fields with any distribution of amplitudes produces a net field that is a very good approximation to Gaussian random, and echo power that is distributed in a chi-square fashion.

The information about EV5's shape and surface scattering is still encoded in the speckles. The speckle distribution tells us that each wavelength-scale spot on the visible surface is radiating independently. Each speckle can be considered an independent sum of the echoes from every one of those spots, added together with different phases determined by the topography of the surface on all scales larger than about 1 cm. In order to determine the phases uniquely, we would need a shape model of the asteroid accurate to 1 cm. Such a model would have $>>10^7$ parameters for EV5. To solve for such a model, we would need to have measured the strength of $>>10^7$ speckles. Since each speckle lasted 0.6 s, measuring $>>10^7$ speckles would have equaled several telescope-months of time, which is impossible to arrange during a radar experiment.

For all but the very smallest (few-meter) and fastest rotating (rotation periods of minutes) radar targets, it is impossible to obtain shape information from the speckle pattern. For these very small targets, a few telescope-hours ($\sim 10^4$ speckles) would provide enough information for a shape model. Such a model would have <10 cm resolution, far better than delay-Doppler imaging.

Supplementary Material 2: Speckles and Interferometric Imaging

While we have applied radar speckle tracking to obtain 2008 EV5's pole direction, we originally attempted a different technique: aperture-synthesis interferometry. A standard technique in radio astronomy, interferometry cross-correlates the signals received at pairs of stations to reconstruct a plane-of-sky image of the target object with resolution $\approx \lambda/$(maximum baseline length). Since longer baselines provide higher resolution, interferometric arrays have become very large, with the Very-Long-Baseline Array containing baselines up to 8000 km (e.g. Taylor et al. 1999).

de Pater et al. 1994 used the 35-km Very Large Array to obtain marginally resolved images of the main-belt radar targets Bamberga and Iris. By constructing images at different frequencies, they were able to obtain those asteroids' pole directions (the portion of a target moving towards the Earth is relatively blueshifted compared to that moving away). Since then, there have been several attempts to extend interferometric imaging to near-Earth asteroid targets, which have much smaller diameters and angular sizes and therefore would require very-long-baseline interferometry (Black et al. 2005, Busch et al. 2008). All of these attempts failed due to the targets' radar speckle patterns. This was not recognized at the time.

Interferometry assumes (Taylor et al. 1999) that the only difference in the plane-of-sky brightness distribution (the image) as seen by two different antennas is the different path lengths between them and the source. A radar speckle pattern violates this assumption: the echo power at one station can have a very different amplitude and phase than at one quite nearby.

There are two possible solutions to this. Either the stations can be placed so close together that they see the same speckles, or each integration can average over many speckles. The former causes an obvious problem: the speckle scale is equal to the baseline length necessary to resolve the

object, preventing imaging. The latter is possible, but only for relatively small arrays and very short speckle durations.

The Earth's atmosphere is variable, and changes the travel time for the signal coming from the source to each antenna, producing path differences and hence phase errors that prevent imaging. With sufficiently strong sources, it is possible to solve for the atmospheric time lags and correct for them (a process called self-calibration, Taylor et al. 1999). For very-long-baseline interferometry at gigahertz frequencies, self-calibration solutions must be computed on 10-s timescales. For small arrays, up to tens of kilometers across, the weather over the antennas is strongly correlated, and self-calibration is possible with longer integration times.

The echo power can vary by up to 100% between one radar speckle and the next. To average the variations to down ~10% takes roughly 100 speckles. For most near-Earth asteroid targets, this takes ~100 s, by which time the atmosphere has changed over an array large enough to resolve them and self-calibration is impossible. Near-Earth asteroids cannot be resolved with interferometry, although astrometry remains possible (e.g. de Pater et al. 1994).

For main-belt radar targets, which have much lower speckle duration and can be imaged with smaller arrays due to their larger sizes, averaging is possible and self-calibration can yield images – as de Pater et al. demonstrated. Unfortunately, only a few main-belt asteroids provide radar echoes strong enough to be imaged with current interferometers.

Additional References

de Pater, I., Palmer, P., Mitchell, D.L., Ostro, S.J., Yeomans, D.K., Snyder, L.E., 1994. Radar aperture synthesis observations of asteroids. Icarus **111**, 489-502.

Taylor, G.B., Carilli, C.L., Perley, R.A., editors. 1999. Synthesis imaging in radio astronomy II. Ast. Soc. Pac. Con. Series, **180**.

Supplementary Table 1: Full List of Antennas for Speckle Tracking

Antennas

Name	*Country*	*Location*	*Diameter (m)*	$A_{Effective}$ (m^2)	*Notes*
Arecibo	USA	18º21′N 66º45′W	305	40000	Fixed dish, works within 20º of zenith (Goldsmith 1996)
Cambridge	UK	52º10′N 0º02′E	32	560	Merlin (Anderson & Davies 1994)
Canberra	Australia	35º24′S 148º59′E	70	2100	Deep Space Network (Imbriale 2003)
Darnhall	UK	53º09′N 2º32′W	25	304	Merlin (Anderson & Davies 1994)
Defford	UK	52º05′N 2º08′W	25	304	Merlin (Anderson & Davies 1994)
DSS-13	USA	35º15′N 116º48′W	34	635	Deep Space Network (Imbriale 2003)
DSS-24,25,26	USA	35º20′N 116º52′W	34	635	Deep Space Network. 3 antennas within 500 m of each other. (Imbriale 2003).
Effelsberg	Germany	50º31′N 6º53′E	100	4150	(Max-Planck Institute 2010)
Fort Davis	USA	30º38′N 103º57′W	25	304	VLBA (Napier et al. 1994)
Green Bank	USA	38º26′N 79º50′W	100	6300	(Minter 2010)
Goldstone DSS-14	USA	35º26′N 116º53′W	70	2100	Deep Space Network (Imbriale 2003)
Hancock	USA	42º56′N 71º59′W	25	304	VLBA (Napier et al. 1994)
Jodrell Bank 26	UK	53º14′N 2º19′W	26	300	Merlin (Anderson & Davies 1994)
Jodrell Bank 76	UK	53º14′N 2º18′W	76	3175	Merlin (Anderson & Davies 1994)
Kashima	Japan	35º57′N 140º39′E	34	450	
Kitt Peak	USA	31º57′N 111º37′W	25	304	VLBA (Napier et al. 1994)
Knockin	UK	52º47′N 3º00′W	25	304	Merlin (Anderson & Davies 1994)
Los Alamos	USA	35º47′N 106º15′W	25	304	VLBA (Napier et al. 1994)
Medicina	Italy	44º31′N 11º39′E	32	450	
Mt. Pleasant	Australia	42º48′S 147º26′E	26	300	
Nobeyama	Japan	35º56′N 138º28′E	45	800	
Noto	Italy	36º53′N 14º59′E	32	450	
Onsala	Sweden	57º24′N 11º55′E	25	275	
Owens Valley 25	USA	37º14′N 118º17′W	25	304	VLBA (Napier et al. 1994)
Owens Valley 40	USA	37º14′N 118º17′W	40	700	
Parkes	Australia	33º00′S 148º16′E	64	1750	
Pickmere	UK	53º17′N 2º27′W	25	304	Merlin (Anderson & Davies 1994)
Pie Town	USA	34º18′N 108º07′W	25	304	VLBA (Napier et al. 1994)
St. Croix	USA	17º45′N 64º35′W	25	304	VLBA (Napier et al. 1994)
Torun	Poland	53º06′N 18º34′E	32	450	
Ventspils	Latvia	57º33′N 21º51′E	32	450	
Usuda	Japan	36º11′N 138º29′E	64	1600	
VLA / EVLA	USA	34º05′N 107º37′W	25	304	27 antenna array <=35 km across. Location array center (Perley et al. 2009)
Westerbork	Netherlands	52º55′N 6º36′E	25	220	14 antenna array 2.3 km across. Location at array center (Baars & Hooghoudt 1974)

This list contains all antennas that could be used for speckle tracking. Those antennas without receivers at the wavelengths of the Arecibo or Goldstone radars and those smaller than 25 m have been excluded. Locations are accurate to 1 km. $A_{Effective}$ values are based on aperture efficiencies at or near 12.6 cm (2.38 GHz). Where multiple identical antennas are at one location, the $A_{Effective}$ given is for a single dish. $A_{Effective}$ estimated from telescope parameters given in Salter (2002) and uncertain by ±20% unless otherwise cited.

Note that special preparation for speckle observations would be required at some of these stations, particularly Effelsberg.

Antenna Pairs		**Separation (km)**	**Sensitivity/VLBA**
Goldstone DSS-14	DSS-24,25,26	10	2.8
Jodrell Bank 26	Pickmere	11	1.0
Jodrell Bank 76	Pickmere	11	1.3
DSS-13	DSS-24,25,26	12	1.9
Pickmere	Darnhall	16	1.0
Jodrell Bank 76	Darnhall	17	1.3
Jodrell Bank 26	Darnhall	18	1.0
Goldstone DSS-14	DSS-13	22	2.8
Usuda	Nobeyama	28	3.3
Knockin	Darnhall	51	1.0
Pie Town	VLA	52	1.0
Pickmere	Knockin	67	1.0
Jodrell Bank 26	Knockin	68	1.0
Jodrell Bank 76	Knockin	68	1.4
Knockin	Defford	96	1.0
Darnhall	Defford	120	1.0
Jodrell Bank 26	Defford	126	1.0
Jodrell Bank 76	Defford	127	1.3
Pickmere	Defford	134	1.0
Cambridge	Defford	149	1.2
Nobeyama	Kashima	197	1.8
Cambridge	Jodrell Bank 26	198	1.2
Jodrell Bank 76	Cambridge	198	2.6
Usuda	Kashima	200	2.0
Cambridge	Darnhall	206	1.2
Cambridge	Pickmere	209	1.2
Cambridge	Knockin	217	1.2
Los Alamos	VLA	226	1.0

Goldstone DSS-14	Owens Valley 40	233	3.1
Goldstone DSS-14	Owens Valley 25	232	1.4
Pie Town	Los Alamos	236	1.0
Arecibo	St. Croix	238	1.4
DSS-13	Owens Valley 40	240	2.2
DSS-13	Owens Valley 25	240	1.3
DSS-24,25,56	Owens Valley 25	250	1.3
DSS-24,25,26	Owens Valley 40	251	2.2
Effelsberg	Westerbork	266	1.0
Canberra	Parkes	274	6.3
Pie Town	Kitt Peak	417	1.0
Kitt Peak	VLA	441	1.0
Cambridge	Westerbork	453	1.0
Effelsberg	Cambridge	510	2.6
Fort Davis	VLA	515	1.0
Torun	Ventspils	538	1.5
Pie Town	Fort Davis	564	1.0
Ventspils	Onsala	585	1.1
Jodrell Bank 76	Westerbork	597	1.0
Los Alamos	Fort Davis	608	1.0
Goldstone DSS-14	Kitt Peak	616	1.4
Torun	Onsala	636	1.1
Kitt Peak	Los Alamos	652	1.0
Effelsberg	Defford	652	1.4
Effelsberg	Jodrell Bank 26	699	1.4
Effelsberg	Jodrell Bank 76	700	11.7
Effelsberg	Pickmere	710	1.4
Effelsberg	Darnhall	711	1.4
Effelsberg	Knockin	727	1.4
Kitt Peak	Fort Davis	744	1.0
Effelsberg	Medicina	757	2.1
Goldstone DSS-14	Pie Town	800	1.4
Green Bank	Hancock	829	1.4
Effelsberg	Onsala	831	1.3
Canberra	Mt. Pleasant	832	1.4
Owens Valley 40	Kitt Peak	845	1.3
Owens Valley 25	Kitt Peak	845	1.0

Kitt Peak	Owens Valley	845	1.0
Effelsberg	Torun	854	2.1
Medicinia	Noto	893	1.5
Cambridge	Onsala	957	1.1
Goldstone	Los Alamos	960	1.4
Owens Valley 40	Pie Town	973	1.3
Owens Valley 25	Pie Town	973	1.0

Pairs of antennas for radar speckle tracking sorted by separation (maximum baseline length). The separations given here have been rounded to the nearest 1 km and are the straight-line distances between the antennas. During an observation, the baseline length decreases depending on the direction to the target, due to foreshortening. Sensitivities are given as ratios of (speckle correlation SNR for antenna pair)/(speckle correlation SNR for two VLBA stations) for the same target and are approximate. This list includes only antenna pairs with baselines less than 1000 km. The preferred baseline length depends on the target object (see text).

When the VLA / EVLA is in its 35-km or 11-km configurations, the baselines between the array's antennas can be used for speckle tracking, with a sensitivity equal to that of VLBA station pairs. These baselines have not been included in this table in the interest of brevity.

References

Anderson, B., Davies, R.D., 1994. Results with the extended MERLIN, Proc. 158th IAU Symp., 343-345.

Baars, J.W.M., Hooghudt, B.G., 1974. The synthesis radio telescope at Westerbork: general lay-out and mechanical aspects. A&A **31**, 323-331.

Goldsmith, P.F., 1996. The second Arecibo upgrade. IEEE Potentials **15**, 38-43.

Imbriale, W.A., 2003. Large antennas of the Deep Space Network. John Wiley & Sons., Hoboken.

Max Planck Institute, 2010. 100m Efflesberg radio telescope calibration parameters, available at http://www.mpifr-bonn.mpg.de/div/effelsberg/.

Minter, T., 2010. The proposer's guide for the Green Bank Telescope. National Radio Astronomy Observatory, available at http://gb.nrao.edu.

Napier, P.J., Bagri, D.S., Clark, B.G., Rogers, A.E.E., Romney, J.D., Thompson, A.R., Walker, R.C., 1994. The Very Long Baseline Array, IEEE Proceedings **82**, 658-672.

Perley, R., and 11 colleagues, 2009. The Expanded Very Large Array, IEEE Proceedings **97**, 1448-1462.

Salter, C.J., 2002. Single-dish radio telescopes of the world. ASP Conf. Proc. 278, 493-503.